# Design Aspects in Photonic Crystal –Vertical Cavity Surface-Emitting Lasers Diode

**Dr. Thaira Zakaria Al-Tayyar & Dr. Raad Sami Fyath****

Received on: 9/6/2010
Accepted on: 7/10/2010

**Abstract**

The design issues for a current injection vertical cavity surface-emitting lasers (VCSEL) operating at 1550 nm is presented using photonic crystal (PC) technology. The design is based on PC slab containing multihole rings with a single defect is introduced at the center which acts as a waveguiding core.

**Keywords:** photonic crystal, single-mode, quantum well, distributed Bragg reflector.

## مقترحات لتصميم ثنائي ليزر عمودي ذو انبعاث سطحي باستخدام تقنية البلورة الفوتونية

**الخلاصة**

يقدم البحث اساسيات لتصميم ثنائي ليزر عمودي ذو انبعاث سطحي يعمل بواسطة الحقن الكهربائي وبطول موجي 1550 نانومتر وذلك باستخدام تقنية البلورة الفوتونية. يعتمد التصميم بالاساس على شريحة بلورة فوتونية مكونة من ثقوب على شكل حلقات متعددة تتوسطها شائبة مفتعلة بدون تثقيب تعمل كمرشد موجة للضوء الناتج.

:

## 1. Introduction

Recently, there has been considerable interest in achieving a low-cost scalable method of designing single-mode VCSELs. The PC approach is unique in its "endlessly single-mode" property, which can provide single-fundamental-mode emission with a specific structure independent of wavelength [1]. Since 2003 PC-VCSELs (see Figure 1) are very prospective light sources since they allow for great flexibility in optical design and provide optical confinement in unoxidized materials [2].

Photonic crystals are materials where a spatially periodic modulation of the dielectric constant affects the properties of photons in a manner analogous to the influence of a semiconductor crystal lattice on the properties of electrons. A high-index two-dimensional (2D) PC contrast is used to form a micro-resonator that simultaneously provides [3]

i) Feedback for laser action.
ii) Diffracts light vertically from the surface.

Advanced functions and high performance, such as thresholds, emission frequencies, linewidths, and beam qualities, are associated with the modal properties of the laser cavity [4] and are realized through quantum well (QW) lasers, distributed Bragg

* Electrical and Electronic Engineering Department, University of Technology/Baghdad
** Engineering College, University of Al-Nahrain /Baghdad



https://doi.org/10.30684/etj.28.24.12
2412-0758/University of Technology-Iraq, Baghdad, Iraq

reflector (DBR) and PC lasers following the development of Fabry-Perot (FP) lasers. Thus the modal control has always been a key issue in developing new types of semiconductor lasers.

Recently nano-scale semiconductor PCs, have been used in very interesting applications such as surface-emission of light. In a PC defect laser, surface emitting in-plane confinement is fully provided by the Bragg reflections from the PC, as shown in Figure 2 [5]. By patterning a high refractive index material on the wavelength scale of light with air holes, a PC can be formed. Such periodicity is often created by etching air holes into a planar semiconductor slab, usually by standard lithographic techniques such as electron-beam lithography [6]. The strong periodic variation of the refractive index results in the formation of a band structure for photons. Most importantly the design of PC can be chosen approparitly that there are wavelength ranges in which the photon propagation is forbbiden. The photonic energy gaps can be used to define miniaturized reflectors which may be used as laser mirrors, boundaries of waveguides, filters,… etc. [7].

**2. PC Cavity Model**

Figure 3 shows the distribution of the holes along the total lateral direction of the cavity in a slab photonic crystal (SPC). A single defect is introduced in the center of the cavity. The cavity is modeled here as a defect cavity of length $L_d$ surrounded by two identical DBRs, one at the right and other at the left. The defect length is given by

$$L_d = 2\Lambda - 2r \quad (1)$$

where $\Lambda$ and r, are respectively, the hole pitch and hole radius. The total length of the PC in the lateral direction is given by

$$L_h = L_d + 2L_{eff} \quad (2)$$

where $L_{eff}$ is the effective length of the DBR.

At the beginning, the effective reflectivity $R_{eff}$ and the effective length $L_{eff}$ of the DBR must be obtained. DBR laser design involves minimization of the coupling losses. If $C_0$ is the power coupling efficiency between the DBR and active waveguides, the effective amplitude-reflection coefficient of the DBR is $r_{eff} = C_0\, r_g$, where $r_g$ is the amplitude-reflection coefficient at the junction of the two waveguides (g emphasizes the grating origin of the reflectivity).

The PC laser is modeled as a DBR laser. The DBR laser is used to provide and utilize a single-longitudinal mode of FP cavity. DBR is FP laser whose mirror reflectivity varies with wavelength, where lasing occurs at a wavelength when the reflectivity becomes maximum. The grating period Λ is determined by the device wavelength in the medium and the order of Bragg diffraction used for the DBR. The Bragg condition for the mth-order coupling between forward- and backward-propagation waves is [8]

$$\Lambda = m\lambda/2\bar{\mu} \quad (3)$$

where $\bar{\mu}$ is the effective-mode index and $\lambda/\bar{\mu}$ is the wavelength inside the medium. In general the pitch $\Lambda$ is calculated as

$$\Lambda = \Lambda_1 + \Lambda_2 \quad (4)$$

$\Lambda_1$ and $\Lambda_2$ are air and semiconductor width thicknesses, (see Figure 4)

$$\Lambda_1 = \lambda/4\mu_1 \quad (5a)$$

$$\Lambda_2 = \lambda/4\mu_2 \quad (5b)$$

For InGaAsP photonic crystal laser operating at 1550 nm, we have $\mu_1 = 1$ and $\mu_2$ = 3.4. These values lead to $\Lambda_1$=387.5nm, $\Lambda_2$=114.0nm, and $\Lambda$ =501.5nm. The hole radius $r = \Lambda_1/2$ = 193.75 nm which gives hole to pitch ratio $r/\Lambda$ =0.386. From eqn. 1, $L_d = 695.25\ nm$.

The DBR length $L_M$, equals the corrugation width multiplied by M which is the number of corrugation periods (or the number of PC rings in this work)

$$L_M = M\,\Lambda \quad (6)$$

For $\Lambda = 501.5\ nm$ and M = 5, $L_M$ = 2507.5 n$m$. The index difference on the two sides of the grating

$$\Delta\mu = \mu_2 - \mu_1 \quad (7)$$

The coupling coefficient κ for which the Bragg condition is satisfied and couples the forward and backward propagating waves over the grating region is given by [10]

$$\kappa = k_0\,\Delta\mu\,\frac{\sin(\pi m\Lambda_1/\Lambda)}{\pi m} \quad (8)$$

where $k_0 = \omega/c = 2\pi/\lambda$ is the vacuum wave number.

The effective length of the Bragg region is expressed as [10]

$$L_{eff} = \frac{tan^{-1}(\kappa L_M)}{2\kappa} \quad (9)$$

The phase mismatch $\Delta\beta$ can be expressed as

$$\Delta\beta = \beta - \frac{m\pi}{\Lambda} = \beta - \beta_0 \quad (10)$$

$$\Delta\beta = \delta + \frac{i\bar{\alpha}}{2} \quad (11)$$

the imaginary part of $\Delta\beta$, i.e. the phase mismatch, is positive to account for the material losses inside the DBR medium, and $\bar{\alpha}$ is the corresponding power absorption coefficient. Taking the Bragg wavelength $\lambda_B = m\bar{\mu}\,\Lambda/2$, the mode detuning $\delta$

$$\delta = \bar{\mu}\,k_0 - \beta_0 = \frac{-2\pi\mu_g}{\lambda^2}\,\Delta\lambda \quad (12)$$

where $\Delta\lambda$ is the diffraction from Bragg wavelength: $\Delta\lambda = \lambda - \lambda_B$, and $\mu_g$ is the group refractive index, (for InGaAsP $\mu_g$= 4).

Let q is the complex wave number to be determined from the boundary conditions and it is related to $\Delta\beta$ and $\kappa$ by [11]

$$q = \pm\sqrt{(\Delta\beta)^2 - \kappa^2} \quad (13)$$

The amplitude-reflection coefficient $r_g$ is obtained from [9] (see Appendix

A for details)

$$r_g = |r_g| \exp(i\phi) = \frac{i\kappa \sin(qL_M)}{q\cos(qL_M) - i\Delta\beta \sin(qL_M)} \quad (14)$$

Figure 5 shows the power reflectivity of the lateral DBR of the PC cavity under investigation. The x-axis of this figure denotes the detuning from the Bragg wavelength. The results are reported for different value of number of periods in the DBR. The parameter values used in the simulation, r = 0.35 $\Lambda$ µm and $\Lambda$ = 501.5 nm which yield a Bragg wavelength of 1550 nm. Note that the reflectivity $R_g$ approaches its maximum value when the frequency detuning=zero. Further, $(R_g)_{max}$ approaches 1 when the number of periods exceeds 5. Thus if the PC is designed with number of hole rings = 5 (or more), the quality factor in the lateral direction tends to infinity. The total quality factor of the cavity $Q_T$ is related to the quality factors in the lateral $Q_{\|}$ and in the perpendicular direction $Q_{\perp}$

$$\frac{1}{Q_T} = \frac{1}{Q_{\|}} + \frac{1}{Q_{\perp}}$$

When $Q_{\|}$ tends to infinity, the cavity quality factor $Q_T$ is then determined by $Q_{\perp}$ which corresponds to the optical losses through the top and bottoms DBRs of the laser structure.

**3. Simulation Results:**

Simulation results are presented for a single-defect PC-VCSEL. The laser is assumed to be design for 1550 nm operation using InGaAsP/InP material system. The parameters values in the simulation are listed in Table 1.

The volume of the cavity is calculated as

$$V_p = \frac{\pi}{4}\left[2L_{eff} + L_d\right]^2 . L \quad (15)$$

where L is the length of the cavity in the perpendicular direction. For five-hole rings considered here, $L_{eff} = 340\ nm$, and $L_d = 615.5\ nm$. For $L = \lambda/2\,\mu_s = 228\ nm$ ( $\mu_s = 3.4$ is the refractive index of the semiconductor material), the volume of the optical cavity becomes $0.30\ \mu m^3$.

The simulation results reveal that the threshold current of this PC-VCSEL is 0.916mA. Figure 6 shows the frequency response when the laser is intensity modulated. The bias current is set to 6mA to yield 2mW emitting power per facet. The y-axis denotes the relative intensity modulation calculated as

$$10 \log\left[\mathrm{H}(f_m)/\mathrm{H}(0)\right],$$

where $f_m = \omega_m/2\pi$.

Note that the intensity modulation approaches a maximum value at modulation frequency $f_m = 45\ GHz$ which corresponds to the resonance frequency of the laser.

The simulation results are compared with those related to a conventional VCSEL designed with cavity diameter equal to 5µm. In this structure, the threshold current is equal to 11.6mA. The frequency response of this laser is also shown in Figure 6. The intensity modulation peaks at $f_m = 23\ GHz$, which indicates a lower speed of operation compared with the PC-VCSEL. The static operation of the

conventional laser reveals that it has a threshold current $I_{th}$ of 11.6mA compared with 0.916mA for the PC-VCSEL.

**4. Conclusions**

The modal behavior and small-signal dynamic characteristics of a 1550nm PC-VCSEL have been investigated theoretically. The main conclusions drawn from this work are

(i) The resonance frequency of the PC cavity is an increasing function of the radius of the inner ring.

(ii) A threshold current of 0.916mA is achieved in the single-defect PC-VCSEL and this to be compared with 11.6mA for a 5μm-diameter conventional VCSEL.

(iii) A high speed operation is expected with PC-VCSELs compared with conventional counterparts. Resonance frequencies of 45GHz and 23GHz are obtained with PC-laser and conventional laser, respectively.

**References**

[1] R. Colombelli, K. Srinivasan, M. Troccoli, O. Painter, C. F. Gmachl, D.M. Tennant, A. M. Sergent, D. L. Sivco, A. Y. Cho, and F. Capasso, "Quantum cascade surface-emitting photonic crystal laser", Science, vol. 302, no. 21, pp. 1374-1377, November 2003.

[2] T. Czyszanowski, M. Dems, and K. Panajotov , "Optimal parameters of photonic-crystal vertical-cavity surface-emitting diode lasers" , Journal of Lightwave Technology, vol. 25, no. 9, pp. 2331-2336, September 2007.

[3] K. Srinivasan and O. Painter, "Fourier space design of high-Q cavities in standard and compressed hexagonal lattice photonic crystals", Optics Express, vol. 11, no. 6, pp. 579-593, March 2003.

[4] J. Piprek and John E. Bowers, "Analog modulation of semiconductor lasers", University of California, Santa Barbara, pp. 57-79, 2000.

[5] N. Yokouchi, A. J. Danner, and K. D. Choquette, "Two-dimensional photonic crystal confined vertical-cavity surface-emitting lasers", IEEE Journal of Selected Topics In Quantum Electronics, vol. 9, no. 5, pp. 1439-1445, September/October 2003.

[6] R. Perahia, K. Srinivasan, O. Painter, V. Moreau, M. Bahriz, R. Colombelli, and F. Capasso , "Quantum cascade photonic crystal lasers: design, fabrication, and applications" ,Optofliudics, vol. 140, no.5, pp.1-2, 2006.

[7] L. Ferrier, P. Rojo-Romeo, E. Drouard, X. Letartre, and P. Viktorovitch, "Slow Bloch mode confinement in 2D photonic crystals for surfaceoperating devices", Optics Express, vol. 16, no. 5, pp. 3136- 3145, March 2008.

[8] N. Yokouchi, A. J. Danner, and K. D. Choquette, "Two-dimensional photonic crystal confined vertical-

cavity surface-emitting lasers", IEEE Journal oF Selected Topics In Quantum Electronics, vol. 9, no. 5, pp. 1439-1445, September/October 2003.

[9] T. E. Murphy, "Design, fabrication and measurement of integrated bragg grating optical filters", PhD Thesis, Massachusetts Institute of Technology, 2001.

[10] L.A. Coldren and S.W. Corzine, "Diode lasers and phonic integrated circuits", University of California-Santa Barbara, John Willy and Sons, 1995.

[11] G. P. Agrawal and N. K. Dutta, "Long-wavelength semiconductor lasers", AT and T Bell Laboratories, Murray Hill, New Jersey, 1986.

**Table 1 : Parameters values used in the simulation.**

| Parameter | Symbol | Value |
|---|---|---|
| Operating wavelength | $\lambda$ | 1550 $nm$ |
| Hole pitch (lattice constant) | $\Lambda$ | 501.5 $nm$ |
| Hole radius | r | 193.75 $nm$ |
| Number of hole rings | M | 5 |
| Semiconductor refractive index | $\mu_s$ | 3.4 |
| Semiconductor group refractive index | $\mu_g$ | 4 |
| Number of QWs | $N_Q$ | 4 |
| QW thickness | $L_z$ | 10 $nm$ |
| Reflectivity of the front and back DBRs | $R_f$ and $R_b$ | 0.98 |
| Length of vertical cavity | L | $\lambda/2\mu_s = 228\ nm$ |
| Defect cavity of length | $L_d$ | $615.5\ nm$ |
| Optical confinement factor | $\Gamma$ | $\left[N_Q.L_z/L\right] = 0.175$ |
| Internal cavity loss | $\alpha_{in}$ | 30 $cm^{-1}$ |
| Gain constant | $a_g$ | $2.5 \times 10^{-16}\ cm^2$ |
| Carrier density at transparency | $n_o$ | $1 \times 10^{18}\ cm^{-3}$ |
| Nonradiative recombination rate | $A_{nr}$ | $1 \times 10^{8}\ s^{-1}$ |
| Radiative recombination coefficient | B | $1.6 \times 10^{-10}\ cm^3/s$ |
| Auger recombination coefficient | C | $5 \times 10^{-29}\ cm^6/s$ |

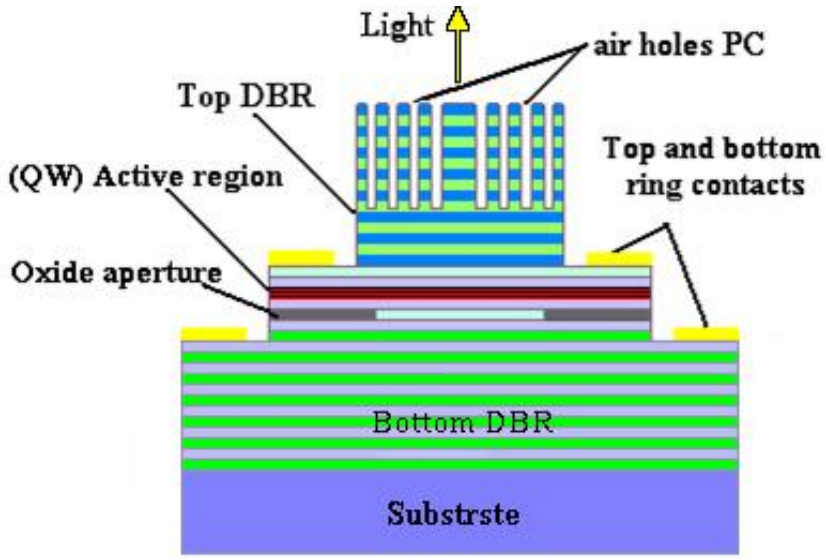


**Figure 1 : A schematic diagram of 2D PC-VCSELs [2].**

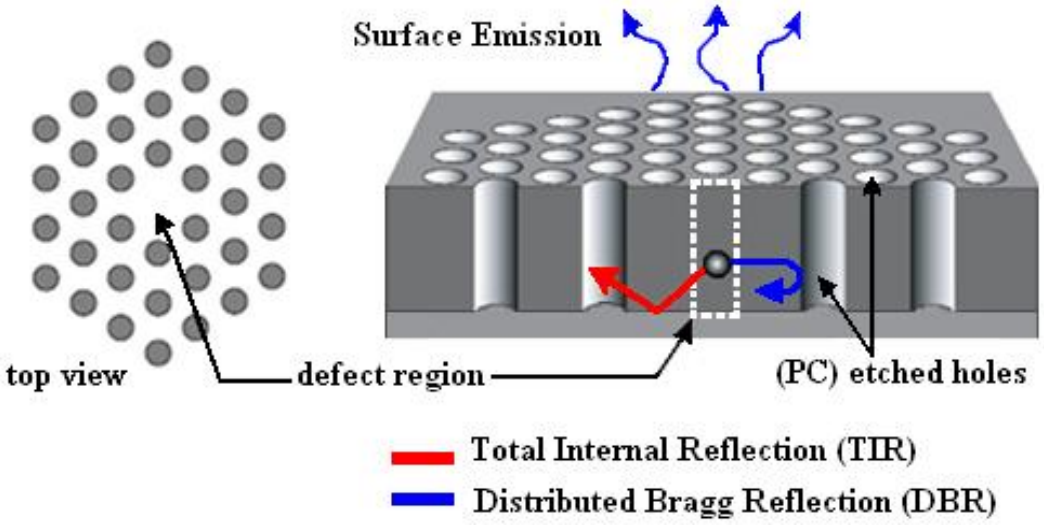


**Figure 2: Vertical emissions in PC surface-emitting laser microcavity [5].**

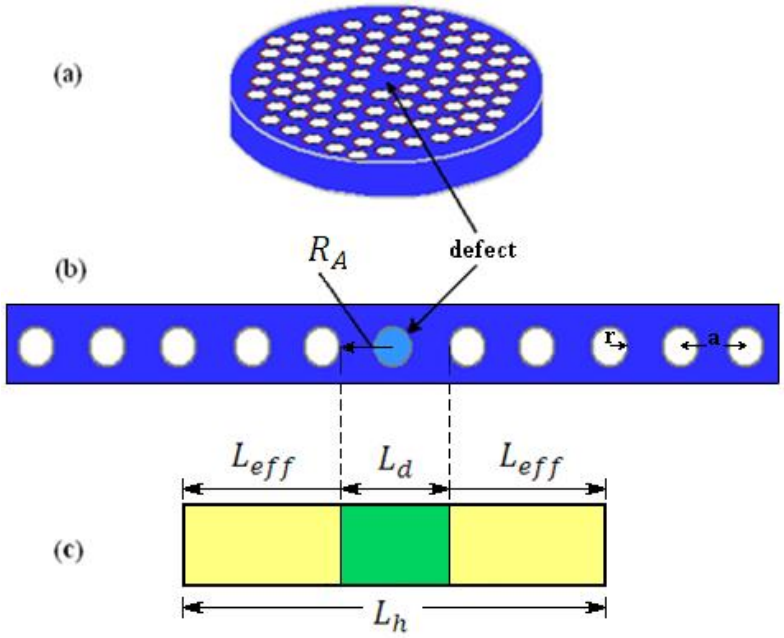


**Figure 3 : Photonic crystal surface emitting laser (PCSEL) model simplification process: (a) 3D view for a 2D SPC PCSEL structure model. (b) Top view of equivalent ideal 2D PC. The diameter of the hole (2r), the distance between the hole axes the pitch (*a*) and the optical aperture ($2R_A$) are defined. (c) DBR model for the PC cavity.**

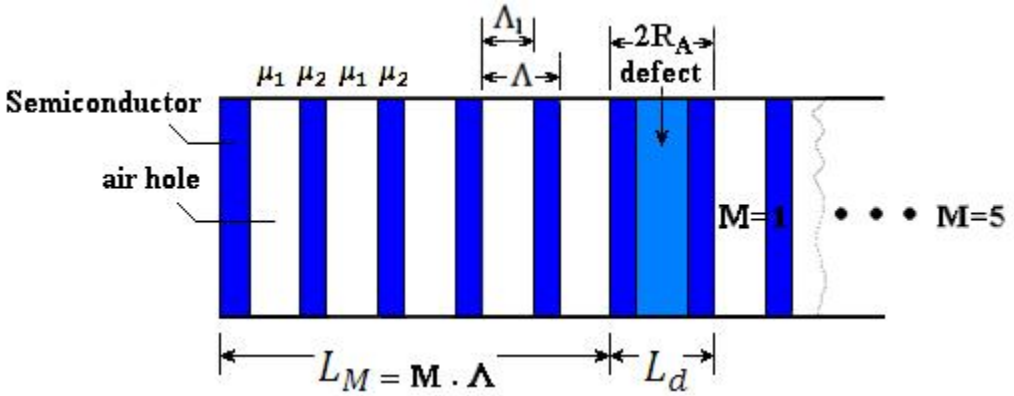


**Figure 4 : Dielectric stack mirror (Bragg grating). Refractive indices $\mu_1 = 1$ for air holes and $\mu_2$ = 3.4 for semiconductor.**

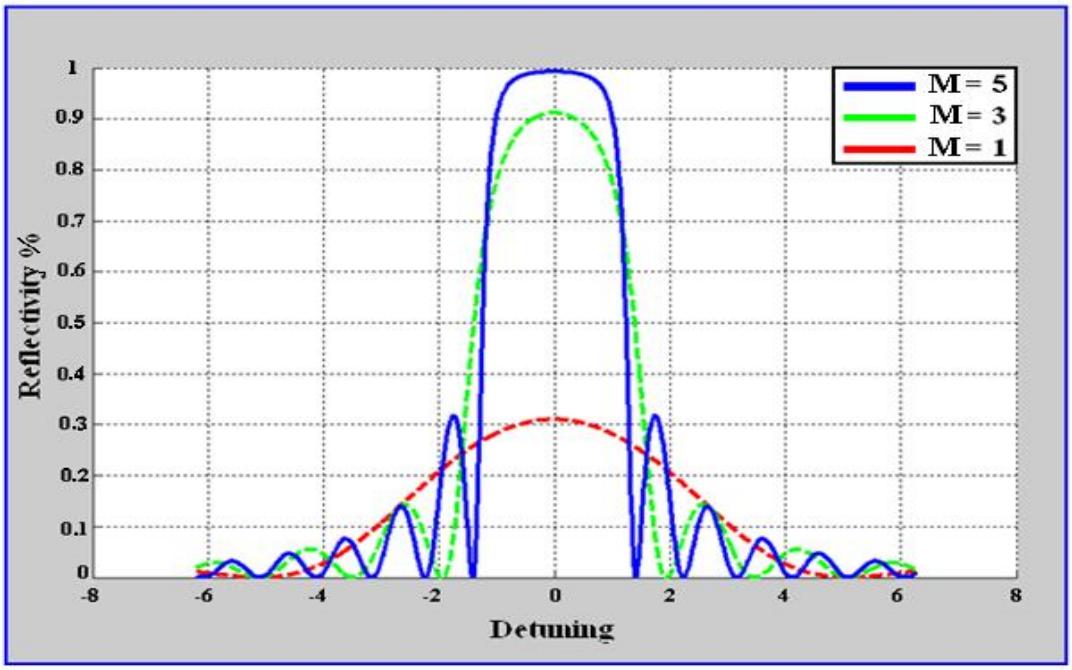


**Figure 5 : Reflectivity of the PC grating as a function of number of hole rings M.**

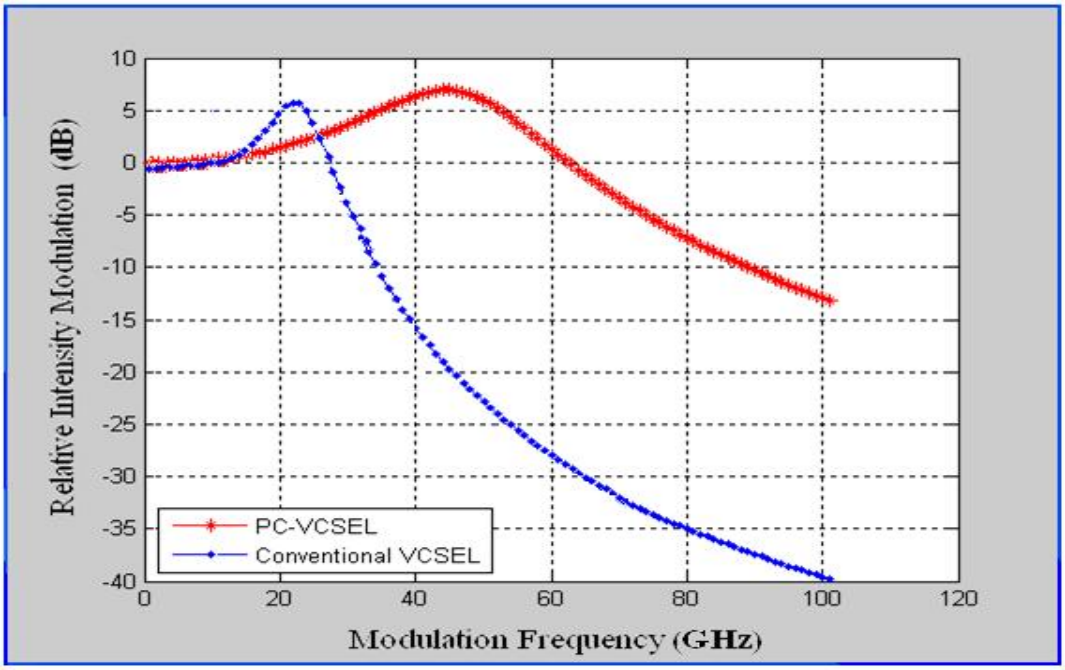


**Figure 6 : Frequency response of the PC-VCSEL under investigation. The results are compared with those related to a conventional VCSEL.**